Central Lancashire Online Knowledge (CLoK)

Title	Environments of strong/ultrastrong, ultraviolet Fe II emitting quasars
Type	Article
URL	https://clok.uclan.ac.uk/8638/
DOI	https://doi.org/10.1093/mnras/stt915
Date	2013
Citation	Clowes, Roger G orcid iconORCID: 0000-0001-8370-465X (2013) Environments of strong/ultrastrong, ultraviolet Fe II emitting quasars. Monthly Notices Of The Royal Astronomical Society, 433 (3). pp. 2467-2475. ISSN 0035-8711
Creators	Clowes, Roger G

Environments of strong/ultrastrong, ultraviolet Fe II emitting quasars

Roger G. Clowes,[1]★ Srinivasan Raghunathan,[2] Ilona K. Söchting,[3]
Matthew J. Graham[4] and Luis E. Campusano[2]

[1]*Jeremiah Horrocks Institute, University of Central Lancashire, Preston PR1 2HE, UK*
[2]*Observatorio Astronómico Cerro Calán, Departamento de Astronomía, Universidad de Chile, Casilla 36-D, Santiago, Chile*
[3]*Astrophysics, Denys Wilkinson Building, Keble Road, University of Oxford, Oxford OX1 3RH, UK*
[4]*California Institute of Technology, 1200 East California Boulevard, Pasadena, CA 91125, USA*

ABSTRACT

We have investigated the strength of ultraviolet (UV) Fe II emission from quasars within the environments of large quasar groups (LQGs) in comparison with quasars elsewhere, for $1.1 \leq \bar{z}_{LQG} \leq 1.7$, using the DR7QSO catalogue of the Sloan Digital Sky Survey. We use the Weymann et al. $W2400$ equivalent width, defined between the rest-frame continuum windows 2240–2255 and 2665–2695 Å, as the measure of the UV Fe II emission. We find a significant shift of the $W2400$ distribution to higher values for quasars within LQGs, predominantly for those LQGs with $1.1 \leq \bar{z}_{LQG} \leq 1.5$. There is a tentative indication that the shift to higher values increases with the quasar i magnitude. We find evidence that within LQGs the ultrastrong emitters with $W2400 \geq 45$ Å (more precisely, ultrastrong plus with $W2400 \geq 44$ Å) have preferred nearest-neighbour separations of $\sim$30–50 Mpc to the adjacent quasar of any $W2400$ strength. No such effect is seen for the ultrastrong emitters that are not in LQGs. The possibilities for increasing the strength of the Fe II emission appear to be iron abundance, Lyα fluorescence and microturbulence, and probably all of these operate. The dense environment of the LQGs may have led to an increased rate of star formation and an enhanced abundance of iron in the nuclei of galaxies. Similarly, the dense environment may have led to more active blackholes and increased Lyα fluorescence. The preferred nearest-neighbour separation for the stronger emitters would appear to suggest a dynamical component, such as microturbulence. In one particular LQG, the Huge-LQG (the largest structure known in the early Universe), six of the seven strongest emitters very obviously form three pairings within the total of 73 members.

Key words: galaxies: active – galaxies: clusters: general – quasars: emission lines – large-scale structure of Universe.

1 INTRODUCTION

From deep MMT/Hectospec spectroscopy to g magnitude $\sim$21, Harris (2011) and Harris et al. (2012) have serendipitously discovered a relative strengthening of ultraviolet (UV) Fe II emission for quasars ($1.1 \leq z \leq 1.7$) in a 2 deg^2 'pencil-beam' field that intersects two large quasar groups (LQGs), U1.11 and U1.28 (Clowes et al. 2012), and a 'doubtful LQG', U1.54. That work suggests that strong/ultrastrong UV Fe II emitters appear to be more strongly represented in dense quasar environments, and that (Clowes & Harris, unpublished visualization) they appear to clump with other quasars or with themselves. Such effects, if confirmed, would be important for our understanding of the origin of the problematic UV Fe II

emission, the influence on it of large- and small-scale environments, and of the evolution of cosmological structures. In this paper, using Sloan Digital Sky Survey (SDSS) spectroscopy, we test whether the above effects are observed when a large sample of LQGs is considered. The pencil-beam study has deep spectroscopy but, of course, narrow-angle coverage. Here, with less deep SDSS spectroscopy, we can consider all of these LQGs in their entirety. We first discuss the statistical properties of the UV Fe II for LQGs in general. We then focus further on these three LQGs U1.11, U1.28, U1.54 together with the 'Huge-LQG', U1.27, of Clowes et al. (2013).

LQGs are the largest structures seen in the early Universe, with sizes $\sim$70–500 Mpc and memberships of $\sim$5–70 quasars. See Clowes et al. (2012, 2013), and earlier references given therein for more details on LQGs. The 'doubtful LQG' U1.54 is a candidate LQG that failed the test of significance described in Clowes et al. (2012), but which had been identified once before as a

★ E-mail: rgclowes@uclan.ac.uk

candidate LQG in an independent survey (Newman et al. 1998; Newman 1999). Sometimes, though, for simplicity we shall refer to this doubtful LQG just as an LQG. Partly, we retain some interest in U1.54 because it and U1.11 and U1.28 are all aligned along the line of sight. The Huge-LQG (U1.27; Clowes et al. 2013) is the largest structure currently known in the early Universe. U1.28, also known as the Clowes & Campusano LQG, (CCLQG; Clowes & Campusano 1991; Clowes et al. 2012) was previously the largest. (In this labelling of the LQGs, 'U' refers to a connected unit, and the appended number gives the mean redshift of its members.)

Iron (Fe) in the optical and UV regions of quasar and AGN spectra is very common, but its occurrence in the UV at the 'ultrastrong' level is rare. A good example of an ultrastrong, UV Fe II emitting quasar is that of Graham, Clowes & Campusano (1996), quasar $2226-3905$. The total number of such ultrastrong quasars known used to be very small, but it has now increased because of the SDSS – for example, Meusinger, Schalldach & Scholz (2012), and our own work. The fractional rate of occurrence remains small; however, we estimate that for redshifts in the range 1.0–1.8, only $\sim$6.6 per cent of all quasars are ultrastrong emitters. [Incidentally, we classify 88 per cent of the high-grade optical and/or UV Fe II emitters with $i \leq 19.1$ and $1.0 \leq z \leq 1.8$ from Meusinger et al. (2012) as strong or ultrastrong UV emitters, and conversely we find a substantially larger total.]

Following Weymann et al. (1991), we use the rest-frame '$W2400$' equivalent width, defined between two continuum windows 2240–2255 and 2665–2695 Å as the index of UV Fe II emission. Based on the median $W2400 \sim 30$ Å for all quasars (non-BAL and BAL) from table 2 of Weymann et al. (1991) we define (Harris 2011; Harris et al. 2012), as an illustrative guide, 'strong emitters' as those with $30 \leq W2400 < 45$ Å and 'ultrastrong' as those with $W2400 \geq 45$ Å. Note, however (see further discussion below), that the sample of $W2400$ values from Weymann et al. (1991) seems to have substantially different properties from ours.

The cause of ultrastrong, UV Fe II emission has not been successfully attributed to any one mechanism, and probably the reality is that several mechanisms contribute, particularly Fe abundance, Lyα fluorescence and microturbulence. Harris (2011) gives a short but detailed review of the current state of understanding. A very brief summary is as follows.

The Fe II is often attributed to the broad-line region (BLR), but there is evidence that it might instead arise from an intermediate-line region, between the outer BLR and the inner torus (e.g. Graham et al. 1996; Zhang 2011). In the early days of trying to understand the Fe II emission, Wills, Netzer & Wills (1985) and Collin-Souffrin & Lasota (1988) concluded that either there was an unusually high abundance of Fe or an important mechanism was being overlooked. Abundance is important, but not likely to be dominant (Sigut & Pradhan 2003; Baldwin et al. 2004). Penston (1987) proposed that Lyα fluorescence might be the overlooked mechanism, with observational and theoretical support following from Graham et al. (1996) and Sigut & Pradhan (1998), respectively. A further important mechanism is microturbulence of $\sim$100 km s^{-1} (Ruff et al. 2012), which increases the spread in wavelength of Fe II absorption (e.g. Bruhweiler & Verner 2008), and thus increases radiative pumping. Strong and ultrastrong Fe II emission might be associated with some special environmental circumstances influencing the quasars.

Harris (2011) and Harris et al. (2012) find that there is a systematic shift by $\sim$9 Å of the $W2400$ equivalent widths to higher values for the 2 deg^2 pencil-beam field that intersects the LQGs U1.11, U1.28 and U1.54 compared with a combined set of 13 2 deg^2 control fields elsewhere. There is then an unusually high rate of occurrence of strong and ultrastrong Fe II emitters. These strong and ultrastrong emitters appear to clump with other quasars or with themselves (Clowes & Harris, unpublished visualization).

From the work of Harris (2011) and Harris et al. (2012) it therefore appears that strong and ultrastrong UV Fe II emitters might preferentially occur where the density of quasars is high, as it is in LQGs. In the case of the pencil-beam field there can be ambiguity about membership of the LQGs by the MMT/Hectospec quasars since they are mostly fainter than the $i \leq 19.1$ quasars from which the LQGs were discovered. The fainter quasars are considered provisionally to be new members primarily if they fall within the convex hull (of member spheres; Clowes et al. 2012) of the existing members. Even so, some are outside the LQGs, although they do still clump – with each other – to form high-density regions. It is possible that these quasars that are outside the LQGs would, with a fainter, wide-angle survey prove to be members too, but with the data currently available there is no way of knowing. It is also possible that the LQG environment itself is not crucial, but that the LQGs are functioning as *providers* of the high (quasar) density environments that favour the Fe II emission. The alignment of these LQGs along the line of sight would then presumably have made the environmental effect prominent and allowed its discovery.

Of 14 strong/ultrastrong quasars in the pencil-beam field, that satisfy the imposed signal-to-noise ratio (s/n) criterion, four are known LQG members (all necessarily from SDSS, but one has also been observed with MMT/Hectospec), five are provisional new members (i.e. they fall within the convex hulls of the LQGs), and five are non-members (all MMT/Hectospec). The one quasar that fails the s/n criterion would be a non-member (from SDSS).

In this paper, we first examine the statistical properties of $W2400$ emission for all of the LQGs with $1.1 \leq \bar{z}_{\text{LQG}} \leq 1.7$ that we have identified in the DR7QSO catalogue (Schneider et al. 2010) for quasars with $1.0 \leq z \leq 1.8$ and $i \leq 19.1$. This allows us to investigate with a much larger sample than that of Harris (2011) and Harris et al. (2012) the $W2400$ properties of LQG members compared with non-members – that is, of quasars that are known to be in dense (quasar) environments compared with those that are not known to be in dense environments. We apply the condition $1.1 \leq \bar{z}_{\text{LQG}} \leq 1.7$ to minimize any 'edge effects' of incomplete membership of the LQGs. We next investigate the distribution of the nearest-neighbour separations of the strongest emitters in the LQGs compared with the weaker emitters in the LQGs. Finally, we focus further on the three LQGs U1.11, U1.28 and U1.54, together with the Huge-LQG, U1.27. We consider here all of the members of these LQGs rather than only those intersected by the pencil beam. The SDSS spectroscopy for these LQGs is, of course, not so deep as the MMT/Hectospec spectroscopy of the pencil beam, but the net outcome is nevertheless a useful increase in the size of the strong/ultrastrong sample.

2 THE LQGs

The LQGs have been discovered in the DR7QSO catalogue (Schneider et al. 2010) using the procedure described fully in Clowes et al. (2012) and summarized briefly in Clowes et al. (2013). Essentially, the procedure involves application of a linkage algorithm followed by a test of statistical significance, the CHMS significance (where CHMS stands for convex hull of member spheres – see Clowes et al. 2012). We restrict the DR7QSO quasars to $i \leq 19.1$ to ensure satisfactory spatial uniformity on the sky, since they are then predominantly from the low-redshift strand of selection (Vanden Berk et al. 2005; Richards et al. 2006). We have selected

Table 1. Properties of the four LQGs U1.11, U1.28, U1.54 (the doubtful LQG) and U1.27. The columns are: the name of the LQG; the number of member quasars; the mean RA, Dec. (2000); the mean redshift; the redshift range; the characteristic size expressed as CHMS volume$^{1/3}$ (see Clowes et al. 2012, 2013 for full details) and references. The total number of member quasars is 166. They all have $i \leq 19.1$, since this limit was imposed on the DR7QSO catalogue (Schneider et al. 2010) to ensure adequate spatial uniformity of the data from which they were discovered. All were discovered within the redshift range $1.0 \leq z \leq 1.8$.

LQG	Members	Mean RA, Dec. (2000)		Mean z	z range	Volume$^{1/3}$ (Mpc)	References
U1.11	38	10:46:13.9	+03:27:10.4	1.11	1.0038–1.2007	380	2
U1.28, CCLQG	34	10:49:10.3	+05:17:09.0	1.28	1.1865–1.4232	350	1, 2
U1.54, doubtful LQG	21	10:55:20.5	+04:45:42.8	1.54	1.4765–1.6136	325	2
U1.27, Huge-LQG	73	10:56:33.0	+14:07:16.9	1.27	1.1742–1.3713	495	3

References: 1 Clowes & Campusano (1991), 2 Clowes et al. (2012) and 3 Clowes et al. (2013).

LQG candidates from quasars within the redshift range $1.0 \leq z \leq 1.8$, but for this work we apply the condition $1.1 \leq \bar{z}_{LQG} \leq 1.7$ to minimize any edge effects of incomplete membership. That is, the LQGs are restricted to $1.1 \leq \bar{z}_{LQG} \leq 1.7$ but the quasars within them are contained by $1.0 \leq z \leq 1.8$.

We consider here LQGs with CHMS significance $\geq 2.8\sigma$ and number of member quasars ≥ 10. The choice of 2.8σ is such that contamination by spurious LQG candidates should be negligible. This selection gives 134 LQGs with $1.0 \leq z \leq 1.8$, incorporating 3092 quasars in total. The smallest membership is 11 and the largest 73 (U1.27, the Huge-LQG). The LQGs are found from within a total of 27 991 quasars. LQG members are thus only $\sim$11 per cent of the total number of quasars. With the further condition $1.1 \leq \bar{z}_{LQG} \leq 1.7$ we have 111 LQGs, incorporating 2629 quasars in total. Again, the smallest membership is 11 and the largest 73. Details of the LQGs will be published in a catalogue paper (Clowes, in preparation).

As mentioned above, the doubtful LQG, U1.54, is not formally a LQG since it fails the test of CHMS significance. It is therefore not one of the above 134/111 LQGs that do pass the test. However, as mentioned above, we retain some interest in U1.54 because it has been identified before as a candidate LQG and because it, U1.11 and U1.28 are all aligned along the line of sight. Also, its CHMS significance is conservative, and, in the case of curved morphology such as U1.54 has, there is therefore the possibility of a candidate LQG being more interesting than is immediately apparent.

We shall focus further on the three LQGs U1.11, U1.28 and U1.54, together with the Huge-LQG, U1.27. These are the LQGs that have so far been investigated in most detail. Their properties are summarized in Table 1.

3 THE W2400 MEASUREMENTS

The member quasars of the LQGs all have $i \leq 19.1$ and all are in the redshift range $1.0 \leq z \leq 1.8$. Recall that to minimize edge effects we are applying the condition $1.1 \leq \bar{z}_{LQG} \leq 1.7$. The rest-frame equivalent width $W2400$, as described by Weymann et al. (1991), has been measured by software written for the purpose. It has been applied to all of the DR7QSO quasars with $i \leq 19.1$ and $1.0 \leq z \leq 1.8$, after smoothing with a five-pixel median filter.

The median filter is used for the following reason. The principal source of error in the $W2400$ measurements seems likely to be the setting of the continuum, given the quite narrow windows of the Weymann method – 15 and 30 Å in the rest frame for the two continuum windows of 2240–2255 and 2665–2695 Å. We have attempted an estimate of the measurement error by comparing the

$W2400$ values arising from the unsmoothed SDSS spectra with those arising from smoothing (in the observed frame) with both a five-pixel (as used in the actual processing) and a nine-pixel median filter. The standard deviation of the difference between them is $\sim$3.5 and 3.7 Å, respectively. The $W2400$ feature itself is so wide that the smoothing of it by the median filter should have a relatively minor effect. We can therefore adopt $\sim$3.5–3.7 Å as an indicative error associated with the $W2400$ measurements. We chose to apply the five-pixel median filter routinely for this purpose of setting the continuum levels more reliably. (The nine-pixel median, however, would increase the effective width of the lower continuum window in particular more than we would wish.)

The median filter also acts to reduce the residual [O I] $\lambda5577$ Å sky feature, for those spectra in which it is present. In most cases, where present, its effect on $W2400$ is smaller than the indicative errors. We can also assume that its occurrence in the LQG sample is identical to that in the matched control sample (see below and the following section).

Approximately 1 per cent of the measurements of $W2400$ by the software are negative. Usually, this happens because the spectra are increasing strongly to the blue, and are therefore concave, leading to negative $W2400$ values, given the rigorous application of the $W2400$ definition. Occasionally, absorption or artefacts in the spectra can also lead to negative values.
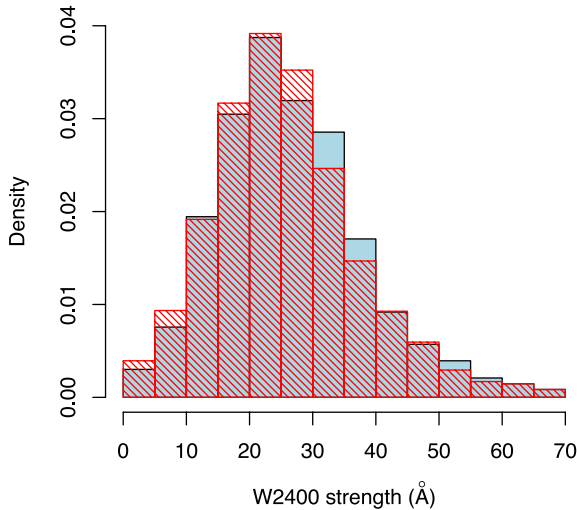
The 3092 LQG members ($1.0 \leq z \leq 1.8$) have been extracted from the entire catalogue to form the LQG sample. The remainder – 24 899 non-LQG-members – of the catalogue is then used as the control sample for comparison. The percentage occurrences of negative $W2400$ are very similar for both the LQG sample and the control sample, and so negative $W2400$ values have simply been removed, leading to final samples of 3063 and 24 604, respectively. Also, one of the 166 members of U1.11, U1.28, U1.54 and U1.27 has negative $W2400$.

For the final control sample, the mean and median $W2400$ values are 26.3 and 25.0 Å, respectively and the standard deviation is 12.2 Å. The mean and median here are thus lower than the median from Weymann et al. (1991) by $\sim$5 Å. The distribution of $W2400$ from Weymann et al. (1991) appears also to be substantially different from ours, having no major symmetrical component and having few low values. We suspect but cannot definitely establish that the Weymann $W2400$ values are systematically too large. Perhaps the quasar sample that they used is not representative of the quasar population. Another possibility is that Weymann et al. used the IRAF SPLOT algorithm, which was changed at about that time, leading to likely differences of $\sim$15 per cent for wide, asymmetrical features (IRAF Newsletter no. 9, 1990). Conceivably, the differences could be larger still for a feature as wide as the Fe II 2400 Å emission.
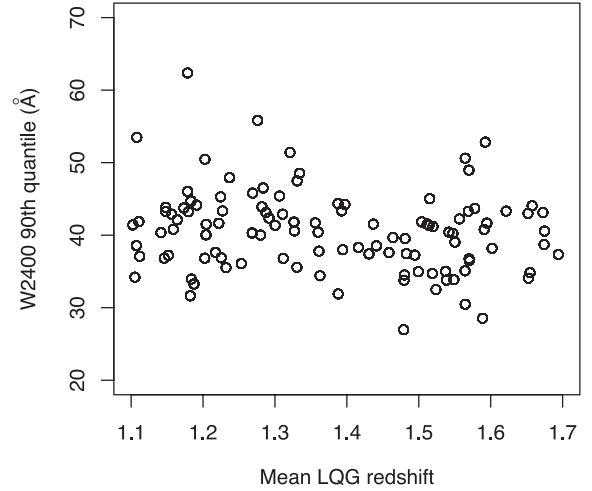
Low-ionization BAL quasars, showing Mg II BAL troughs, can lead to $W2400$ values that are too large, since the continuum for the $W2400$ measurement is then underestimated. Such quasars can be removed using the data base of Shen et al. (2011), but in practice the rate of occurrence is too low to make anything other than a very slight difference to the analysis. The Shen et al. (2011) data base does not allow removal of all problematic Mg II absorption troughs, however, so, for the purpose of statistical analysis, we simply assume that they can be neglected as their rate of occurrence should be the same for both the LQG sample and the control sample. (We also make the same assumption for the sample extracted for U1.11, U1.28, U1.54 and U1.27.)

4 ANALYSIS OF THE W2400 DISTRIBUTION

The distribution of the rest-frame equivalent width, $W2400$, for the 2604 members of the 111 LQGs with $1.1 \leq \bar{z}_{\mathrm{LQG}} \leq 1.7$ is shown in Fig. 1 as the solid histogram. The figure shows in addition the distribution for a matched subset of the control sample as the hatched histogram. The matched subset, intended to negate possible dependences on magnitude and redshift, has been created from the final control sample by finding, for each member of the 111 LQGs, the member of the control sample that is closest in i magnitude and in $10 \times z$, where z is the redshift. The use of $10 \times z$ is so that we give equal weight to an interval of 0.1 in i and 0.01 in z. Both histograms are density histograms (meaning that relative frequency is given by bin height × bin width). Both are for $i \leq 19.1$ and $1.0 \leq z \leq 1.8$, with the condition $1.1 \leq \bar{z}_{\mathrm{LQG}} \leq 1.7$ applied to the LQGs. A one-sided Mann–Whitney test indicates that there is a relative shift of the LQG distribution to larger values at a level of significance given by the p-value $= 0.0226$. The median shift is estimated as 0.62 Å. Note that the histograms of Fig. 1 and subsequent figures are for illustration, and the statistical analysis with the Mann–Whitney test (or Kolmogorov–Smirnov test) does not depend on binned data. If we restrict the i magnitudes of the LQG quasars to $18.0 \leq i \leq 19.1$

Figure 2. A plot of the 90th quantile of the rest-frame equivalent width, $W2400$, distribution against $\bar{z}_{\mathrm{LQG}}$ for the 111 LQGs with $1.1 \leq \bar{z}_{\mathrm{LQG}} \leq 1.7$. Note the apparent change in properties at $\bar{z}_{\mathrm{LQG}} \sim 1.48$.

then the p-value becomes 0.0064 and the median shift becomes 0.84 Å. The shift to higher $W2400$ thus appears to be a stronger effect at fainter magnitudes.

The LQGs appear to show a change in the properties of their $W2400$ distributions at $\bar{z}_{\mathrm{LQG}} \sim 1.48$. This change is illustrated in Fig. 2 which plots, for each LQG with $1.1 \leq \bar{z}_{\mathrm{LQG}} \leq 1.7$, the value of the 90th quantile of the $W2400$ distribution against $\bar{z}_{\mathrm{LQG}}$. The 90th quantile is used to characterize the strong tail of the $W2400$ distribution for each LQG. There appears to be a discontinuity in the typical value of the 90th quantile and in the upper and lower envelopes at $\bar{z}_{\mathrm{LQG}} \sim 1.48$.

Given this change at $\bar{z}_{\mathrm{LQG}} \sim 1.48$, we apply instead the condition $1.1 \leq \bar{z}_{\mathrm{LQG}} \leq 1.5$. It then appears that the shift of the LQG distribution to higher values of $W2400$ is strongly concentrated in this redshift range. Fig. 3 is similar to Fig. 1 but instead gives the distribution of the rest-frame equivalent width, $W2400$, for the

Figure 1. The distribution of the rest-frame equivalent width, $W2400$, is shown for the 111 LQGs with $1.1 \leq \bar{z}_{\mathrm{LQG}} \leq 1.7$ as the solid histogram (2604 quasars). The distribution for the matched control sample (see the text) is shown as the hatched histogram (2604 quasars). Both are density histograms. Both are for $i \leq 19.1$ and $1.0 \leq z \leq 1.8$, with the condition $1.1 \leq \bar{z}_{\mathrm{LQG}} \leq 1.7$ applied to the LQGs. The bin size is 5 Å. As explained in the text, negative $W2400$ values have been removed. The histograms have been truncated at $W2400 = 70$ Å for clarity.
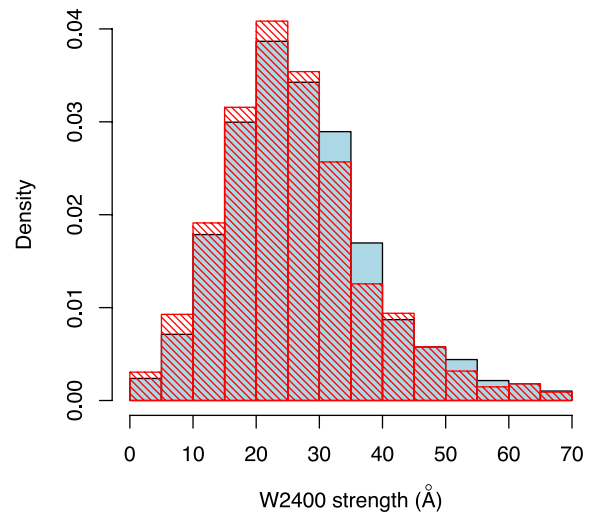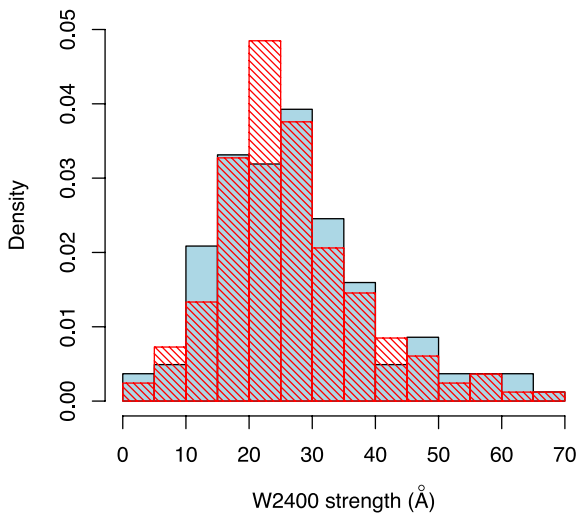

Figure 3. The distribution of the rest-frame equivalent width, $W2400$, is shown for the 75 LQGs with $1.1 \leq \bar{z}_{\mathrm{LQG}} \leq 1.5$ as the solid histogram (1778 quasars). The distribution for the matched control sample (see the text) is shown as the hatched histogram (1778 quasars). Both are density histograms. Both are for $i \leq 19.1$ and $1.0 \leq z \leq 1.8$, with the condition $1.1 \leq \bar{z}_{\mathrm{LQG}} \leq 1.5$ applied to the LQGs. Other details are the same as for Fig. 1.

1778 members of the 75 LQGs with $1.1 \leq \bar{z}_{LQG} \leq 1.5$ as the solid histogram. The hatched histogram shows the distribution for the corresponding matched subset of the control sample. In this case, the one-sided Mann–Whitney test indicates a relative shift of the LQG distribution to larger values at p-value $= 0.0042$. The median shift is estimated as 0.97 Å. Note that this condition $1.1 \leq \bar{z}_{LQG} \leq 1.5$ leads to the member quasars having redshifts in the range $1.0006 \leq z \leq 1.6093$. If we again restrict the i magnitudes of the LQG quasars to $18.0 \leq i \leq 19.1$ then the p-value becomes 0.000 54 and the median shift becomes 1.31 Å. Again, the shift to higher $W2400$ appears to be a stronger effect at fainter magnitudes.

If, having considered the subrange $1.1 \leq \bar{z}_{LQG} \leq 1.5$, we now consider only the remaining $1.5 < \bar{z}_{LQG} \leq 1.7$, then there is no perceptible shift at all of the LQG distribution to higher values of $W2400$. Of course, the number of LQGs and members is then somewhat smaller (36 LQGs, 826 members), but we cautiously conclude that the shift to higher $W2400$ is indeed strongly concentrated in the range $1.1 \leq \bar{z}_{LQG} \leq 1.5$.

In summary so far, we find a small but significant shift to higher values of $W2400$ for LQGs with $1.1 \leq \bar{z}_{LQG} \leq 1.5$. This result contrasts with that from Harris (2011) and Harris et al. (2012) for a large shift for quasars with $1.1 \leq z \leq 1.7$ in the pencil-beam field that intersects the LQGs U1.11, U1.28 and U1.54. However, we do find some indication that the shift that we find here increases to fainter magnitudes. The MMT/Hectospec data used by Harris (2011) and Harris et al. (2012) are for quasars that are typically much fainter than those used here, so it may be that the results can still be reconciled.

Fig. 4 similarly shows the distribution of the rest-frame equivalent width, $W2400$, for the four LQGs U1.11, U1.28 (the CCLQG) and U1.54 (the doubtful LQG), and U1.27 (the Huge-LQG). Their $W2400$ distribution is shown as the solid histogram, and again the distribution for the corresponding matched control sample is shown as the hatched histogram. The one-sided Mann–Whitney test indicates that there is no significant shift to larger values. From the statistics for the 75 LQGs with $1.1 \leq \bar{z}_{LQG} \leq 1.5$ we would, ignoring the different redshift limits arising from the inclusion of U1.54, expect an excess of only 1.6 ultrastrong and 5.8 strong emitters

Figure 4. The distribution of the rest-frame equivalent width, $W2400$, is shown for the four LQGs U1.11, U1.28 (the CCLQG), U1.54 (the doubtful LQG) and U1.27 (the Huge-LQG) as the solid histogram (165 quasars). The distribution for the matched control sample is shown as the hatched histogram (165 quasars). Other details are the same as for Fig. 1.

for these four LQGs (166 quasars, 165 with positive $W2400$). Most probably the signal is lost in the noise.

Note that, very unusually for the DR7QSO catalogue, nine of the 166 spectra for U1.11, U1.27, U1.54 and U1.28 have exposure times of only 900 s. In fact, only U1.11 and U1.28 are affected, with seven of the nine from U1.11 and two from U1.28. Three of the nine are estimated to have s/n < 4 (two from U1.28 and one from U1.11). The software measurements of $W2400$ place two in the ultrastrong category and one in the strong. Manual measurement suggests that, despite the noise, the software measurements are acceptable.

The members of U1.11, U1.28, U1.54 and U1.27 that have been classified as strong or ultrastrong emitters are listed in Table 2. We can briefly compare the classification here with those of Harris (2011) for the small area of the pencil-beam field. The superscripts in the first column of Table 2 give the corresponding classification from Harris (2011) or, for SDSS J104932.22+050531.7, from Harris (private communication). Note that SDSS J104938.35+052932.0 is classified as ultrastrong here and weak in Harris (2011): the software measurement here will be incorrect because of absorption occurring at the position of one of the continuum windows. Two quasars classified as ultrastrong here but strong by Harris are here on the boundary between the ultrastrong and strong classifications. A quasar classified as strong by Harris (2011) but weak by the software measurements, SDSS J104840.34+055912.9 appears on manual checking to be weak.

5 ENVIRONMENTS OF THE ULTRASTRONG UV FE II EMITTERS

In this section, we discuss the environments of the ultrastrong ($W2400 \geq 45$ Å) UV Fe II emitters compared with the weak ($W2400 < 30$ Å) within the 75 LQGs having $1.1 \leq \bar{z}_{LQG} \leq 1.5$. We also briefly discuss the particular LQGs U1.11, U1.28, U1.54 and U1.27. If the shift to higher $W2400$ within the LQGs arises from an environmental effect then we might anticipate there will be a density or clustering effect that appears most strongly for the ultrastrong emitters compared with the weak. There is an arbitrary element to this approach, of course, because the definitions of ultrastrong, strong and weak emitters involve arbitrary boundaries.

Clowes & Harris (unpublished visualization) found that the strong and ultrastrong emitters tended to clump with other quasars or with themselves, both within and outside the convex hulls of the three LQGs U1.11, U1.28 and U1.54. (Recall that the deep MMT/Hectospec spectroscopy in the pencil beam included quasars fainter than the $i \leq 19.1$ limit of the quasars used for the discovery of the LQGs.) Although this visualization involved no quantification of the clumping, it has guided our thinking that there could be a preferred nearest-neighbour scale for the strongest emitters.

For these reasons, we have investigated the distribution of nearest-neighbour separations for the ultrastrong emitters within the LQGs compared with the distribution for the weak emitters within the LQGs. The nearest neighbours have been determined without regard for the strength of their UV Fe II emission. We consider only the LQGs with $1.1 \leq \bar{z}_{LQG} \leq 1.5$, given the earlier result that the shift to higher values of $W2400$ is strongly concentrated in this range.

The distribution of the nearest-neighbour separations (present epoch) for the members of the 75 LQGs with $1.1 \leq \bar{z}_{LQG} \leq 1.5$ and for $W2400 \geq 45$ Å (i.e. ultrastrong) is shown in Fig. 5 as the solid histogram, with mean 57.46 ± 1.70 Mpc. The figure also shows the corresponding distribution for $W2400 < 30$ Å (i.e. weak) as the hatched histogram, with mean 59.65 ± 0.63 Mpc. Both are density histograms. Both are for $i \leq 19.1$ and $1.0 \leq z \leq 1.8$.

Table 2. Strong ($30 \leq W2400 < 45$ Å) and ultrastrong ($W2400 \geq 45$ Å) UV Fe II emitters in the four LQGs U1.11, U1.28, U1.54 and U1.27 The columns are: category (whether strong or ultrastrong); quasar SDSS name; redshift z; RA, Dec. (2000); the name of the LQG; $W2400$ equivalent width and i magnitude.

Category	Quasar SDSS name	z	RA, Dec. (2000)	LQG	W2400 (Å)	i
Ultrastrong	SDSS J104445.32+054348.8	1.1879	10:44:45.32 +05:43:48.8	U1.28 (CCLQG)	74.60	18.793
Ultrastrong[w]	SDSS J104938.35+052932.0	1.5169	10:49:38.35 +05:29:32.0	U1.54 (dou. LQG)	74.25	19.064
Ultrastrong	SDSS J110412.00+044058.2	1.2554	11:04:12.00 +04:40:58.2	U1.28 (CCLQG)	67.30	18.851
Ultrastrong	SDSS J110736.60+090114.7	1.2266	11:07:36.60 +09:01:14.7	U1.27 (Huge-LQG)	62.49	18.902
Ultrastrong	SDSS J105527.67+002001.5	1.1448	10:55:27.67 +00:20:01.5	U1.11	62.17	18.782
Ultrastrong[u]	SDSS J104914.32+041428.6	1.6070	10:49:14.32 +04:14:28.6	U1.54 (dou. LQG)	61.17	18.871
Ultrastrong	SDSS J104509.93+063559.0	1.1184	10:45:09.93 +06:35:59.0	U1.11	59.31	19.001
Ultrastrong	SDSS J110810.87+014140.7	1.6136	11:08:10.87 +01:41:40.7	U1.54 (dou. LQG)	58.04	17.344
Ultrastrong	SDSS J110504.46+084535.3	1.2371	11:05:04.46 +08:45:35.3	U1.27 (Huge-LQG)	55.20	19.005
Ultrastrong	SDSS J104445.03+151901.6	1.2336	10:44:45.03 +15:19:01.6	U1.27 (Huge-LQG)	54.31	18.678
Ultrastrong	SDSS J110121.37+054349.7	1.5252	11:01:21.37 +05:43:49.7	U1.54 (dou. LQG)	53.42	18.746
Ultrastrong	SDSS J103744.89+051834.2	1.2280	10:37:44.89 +05:18:34.2	U1.28 (CCLQG)	52.54	18.958
Ultrastrong	SDSS J104139.15+143530.2	1.2164	10:41:39.15 +14:35:30.2	U1.27 (Huge-LQG)	48.38	18.657
Ultrastrong	SDSS J105224.08+204634.1	1.2032	10:52:24.08 +20:46:34.1	U1.27 (Huge-LQG)	47.74	18.593
Ultrastrong	SDSS J103552.43+032537.2	1.0553	10:35:52.43 +03:25:37.2	U1.11	46.09	18.980
Ultrastrong[s*]	SDSS J104932.22+050531.7	1.1136	10:49:32.22 +05:05:31.7	U1.11	45.72	18.699
Ultrastrong	SDSS J105119.60+142611.4	1.3093	10:51:19.60 +14:26:11.4	U1.27 (Huge-LQG)	45.57	19.002
Ultrastrong[s]	SDSS J105251.71+055733.7	1.5928	10:52:51.71 +05:57:33.7	U1.54 (dou. LQG)	45.11	18.440
Ultrastrong	SDSS J104752.69+061828.9	1.3125	10:47:52.69 +06:18:28.9	U1.28 (CCLQG)	45.07	18.954
Strong[+]	SDSS J105144.88+125828.9	1.3153	10:51:44.88 +12:58:28.9	U1.27 (Huge-LQG)	44.48	19.021
Strong	SDSS J105534.66+033028.8	1.2495	10:55:34.66 +03:30:28.8	U1.28 (CCLQG)	41.25	18.195
Strong	SDSS J110016.88+193624.7	1.2399	11:00:16.88 +19:36:24.7	U1.27 (Huge-LQG)	40.41	18.605
Strong	SDSS J103626.33+045436.4	1.0477	10:36:26.33 +04:54:36.4	U1.11	40.20	18.404
Strong	SDSS J105611.27+170827.5	1.3316	10:56:11.27 +17:08:27.5	U1.27 (Huge-LQG)	39.87	17.698
Strong	SDSS J105537.63+040520.0	1.2619	10:55:37.63 +04:05:20.0	U1.28 (CCLQG)	38.98	18.651
Strong	SDSS J105821.28+053448.9	1.2540	10:58:21.28 +05:34:48.9	U1.28 (CCLQG)	38.87	18.134
Strong	SDSS J104012.14+043904.6	1.1195	10:40:12.14 +04:39:04.6	U1.11	38.57	18.578
Strong	SDSS J105525.68+113703.0	1.2893	10:55:25.68 +11:37:03.0	U1.27 (Huge-LQG)	38.54	18.264
Strong	SDSS J110217.19+083921.1	1.2355	11:02:17.19 +08:39:21.1	U1.27 (Huge-LQG)	37.75	18.800
Strong	SDSS J105141.89+045831.8	1.6080	10:51:41.89 +04:58:31.8	U1.54 (dou. LQG)	37.70	18.906
Strong	SDSS J111823.21+090504.9	1.1923	11:18:23.21 +09:05:04.9	U1.27 (Huge-LQG)	37.65	18.940
Strong	SDSS J105132.22+145615.1	1.3607	10:51:32.22 +14:56:15.1	U1.27 (Huge-LQG)	36.16	18.239
Strong	SDSS J104116.79+035511.4	1.2444	10:41:16.79 +03:55:11.4	U1.28 (CCLQG)	35.74	18.531
Strong	SDSS J103748.36+040242.1	1.0869	10:37:48.36 +04:02:42.1	U1.11	35.56	17.857
Strong	SDSS J105352.72+050043.9	1.1320	10:53:52.72 +05:00:43.9	U1.11	35.39	18.865
Strong	SDSS J105719.23+045548.2	1.3355	10:57:19.23 +04:55:48.2	U1.28 (CCLQG)	35.36	18.429
Strong	SDSS J104656.71+054150.3	1.2284	10:46:56.71 +05:41:50.3	U1.28 (CCLQG)	34.66	17.594
Strong	SDSS J104843.05+064456.8	1.3523	10:48:43.05 +06:44:56.8	U1.28 (CCLQG)	34.55	18.721
Strong	SDSS J104410.13+072305.6	1.1514	10:44:10.13 +07:23:05.6	U1.11	34.51	18.189
Strong	SDSS J104430.92+160245.0	1.2294	10:44:30.92 +16:02:45.0	U1.27 (Huge-LQG)	34.29	17.754
Strong	SDSS J105637.49+150047.5	1.3713	10:56:37.49 +15:00:47.5	U1.27 (Huge-LQG)	33.58	19.041
Strong	SDSS J105833.86+055440.2	1.3222	10:58:33.86 +05:54:40.2	U1.28 (CCLQG)	33.40	18.758
Strong	SDSS J105621.90+143401.0	1.2333	10:56:21.90 +14:34:01.0	U1.27 (Huge-LQG)	33.37	19.052
Strong	SDSS J105832.01+170456.0	1.2813	10:58:32.01 +17:04:56.0	U1.27 (Huge-LQG)	33.36	18.299
Strong	SDSS J105017.31+012450.9	1.2007	10:50:17.31 +01:24:50.9	U1.11	33.07	18.800
Strong	SDSS J104425.80+060925.6	1.2523	10:44:25.80 +06:09:25.6	U1.28 (CCLQG)	32.40	18.652
Strong	SDSS J104114.06+034312.0	1.2633	10:41:14.06 +03:43:12.0	U1.28 (CCLQG)	32.20	18.588
Strong	SDSS J104309.70+075317.8	1.1823	10:43:09.70 +07:53:17.8	U1.11	32.19	18.872
Strong	SDSS J103639.63+022553.5	1.0525	10:36:39.63 +02:25:53.5	U1.11	32.17	18.817
Strong	SDSS J105442.71+104320.6	1.3348	10:54:42.71 +10:43:20.6	U1.27 (Huge-LQG)	31.82	18.844
Strong	SDSS J105022.81+064621.8	1.2900	10:50:22.81 +06:46:21.8	U1.28 (CCLQG)	31.07	18.362
Strong	SDSS J105512.23+061243.9	1.3018	10:55:12.23 +06:12:43.9	U1.28 (CCLQG)	31.00	18.413
Strong	SDSS J105525.18+191756.3	1.2005	10:55:25.18 +19:17:56.3	U1.27 (Huge-LQG)	30.81	18.833
Strong	SDSS J104954.70+160042.3	1.3373	10:49:54.70 +16:00:42.3	U1.27 (Huge-LQG)	30.78	18.748
Strong	SDSS J105541.83+111754.2	1.3298	10:55:41.83 +11:17:54.2	U1.27 (Huge-LQG)	30.57	18.996
Strong	SDSS J105245.80+134057.4	1.3544	10:52:45.80 +13:40:57.4	U1.27 (Huge-LQG)	30.28	18.211

[u]Classified as ultrastrong in Harris (2011).

[s]Classified as strong in Harris (2011).

[s*]Classified as strong (Harris, private communication).

[w]Classified as weak ($W2400 < 30$ Å) in Harris (2011).

[+]This and entries above are classified also as ultrastrong plus ($W2400 \geq 44$ Å) – see the text.
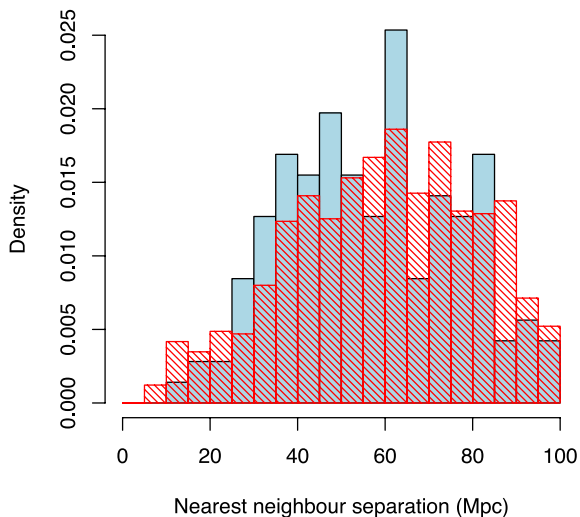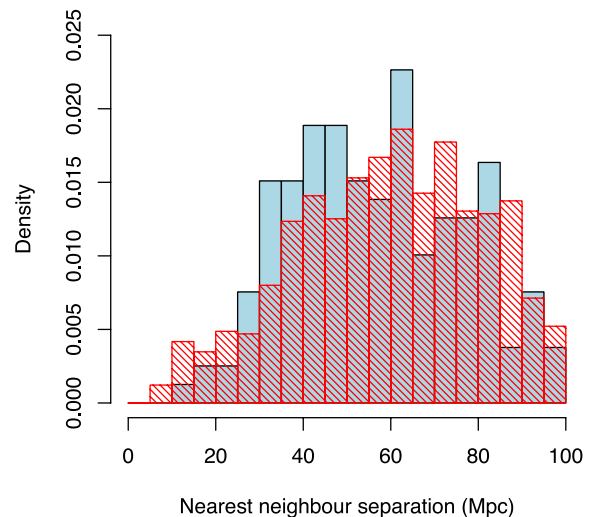
Figure 5. The distribution of the nearest-neighbour separations (present epoch) for the members of the 75 LQGs with $1.1 \leq \bar{z}_{LQG} \leq 1.5$ and for $W2400 \geq 45$ Å (i.e. ultrastrong) is shown as the solid histogram (143 quasars), with mean 57.46 ± 1.70 Mpc. The distribution for the members of the LQGs with $W2400 < 30$ Å is shown as the hatched histogram (1152 quasars), with mean 59.65 ± 0.63 Mpc. Both are density histograms. Both are for $i \leq 19.1$ and $1.0 \leq z \leq 1.8$. The bin size is 5 Mpc. Note the apparent preference of the $W2400 \geq 45$ Å quasars for separations in the range 25–50 Mpc. Note that the LQG-finding algorithm restricts separations to ≤ 100 Mpc.

Although drawn from the same LQGs, the two histograms appear different, with that for $W2400 \geq 45$ Å indicating preferred values of the nearest-neighbour separation predominantly in the range ∼25–50 Mpc (present epoch) – note the consecutive bins where the histogram for $W2400 \geq 45$ Å exceeds the histogram for $W2400 < 30$ Å. A Mann–Whitney test is inappropriate here because the LQG-finding algorithm restricts separations to ≤ 100 Mpc, but a one-sided Kolmogorov–Smirnov test indicates that the cumulative distribution function (CDF) of the $W2400 \geq 45$ Å distribution is greater than the CDF of the $W2400 < 30$ Å distribution, with p-value = 0.0255, which is marginally significant.

Given the arbitrary boundaries for the definitions of ultrastrong, strong and weak emitters we note that a post-hoc adjustment from $W2400 \geq 45$ Å to $W2400 \geq 44$ Å gives the histograms shown in Fig. 6, with means 57.40 ± 1.60, 59.65 ± 0.63 Mpc, and the Kolmogorov–Smirnov test gives a p-value = 0.0197. The preferred nearest-neighbour separation appears then to be predominantly in the range ∼30–50 Mpc.

Although we find evidence for a preferred nearest-neighbour scale for the ultrastrong-emitting quasars in LQGs we find no evidence for a preferred scale in the quasars that are not members of LQGs (mean nearest-neighbour separation ∼78 Mpc), across a comparable range of redshifts. Thus, the preferred nearest-neighbour scale of ∼30–50 Mpc for the $W2400 \geq 45$ Å (more precisely, $W2400 \geq 44$ Å) emitters seems to be peculiar to the LQG environment. Presumably, it is related to the shift to higher $W2400$ values within the LQGs.

We have similarly used the visualization software to look at the environments of the strongest emitters from the entire memberships of the same three LQGs from Harris (2011) and Harris et al. (2012), U1.11, U1.28 and U1.54, together with U1.27. Given the above result on the nearest-neighbour separations we concentrate on the quasars with $W2400 \geq 44$ Å rather than simply $W2400 \geq$


Figure 6. The distribution of the nearest-neighbour separations (present epoch) for the members of the 75 LQGs with $1.1 \leq \bar{z}_{LQG} \leq 1.5$ and for $W2400 \geq 44$ Å (post-hoc adjustment) is shown as the solid histogram (160 quasars), with mean 57.40 ± 1.60 Mpc. The distribution for the members of the LQGs with $W2400 < 30$ Å is shown as the hatched histogram (1152 quasars), with mean 59.65 ± 0.63 Mpc. Both are density histograms. Both are for $i \leq 19.1$ and $1.0 \leq z \leq 1.8$. The bin size is 5 Mpc. Note the apparent preference of the $W2400 \geq 44$ Å quasars for separations in the range 30–50 Mpc. Note that the LQG-finding algorithm restricts separations to ≤ 100 Mpc.

45 Å. To simplify the discussion we introduce an ultrastrong-plus category as those with $W2400 \geq 44$ Å (while still retaining 'ultrastrong' as those with $W2400 \geq 45$ Å). The findings are similar to those previously, but not always so clear, perhaps because of the brighter limiting magnitude. For example, with U1.54, the doubtful LQG, only two of the five ultrastrong-plus emitters appear to be closely associated with other quasars, and only one of these is in a dense region. In contrast, with U1.11, three of four ultrastrong-plus emitters do seem to be associated with other quasars and denser regions. With U1.28, two of four ultrastrong-plus emitters appear to be close to other quasars, but with neither being in particularly dense regions. With U1.27 (the Huge-LQG), six of the seven ultrastrong-plus emitters form three pairs (separations 52, 81, 105 Mpc), within the total membership of 73. One pairing is actually part of a close triplet with another quasar in a generally dense region, and another pairing is part of a looser triplet in a less dense region. The third pairing has one quasar in a dense region and the other detached from it. The seventh ultrastrong-plus quasar is close to another quasar in a less dense region. A visualization of the location of these seven ultrastrong-plus emitters within U1.27 is shown in Fig. 7.

6 DISCUSSION AND CONCLUSIONS

We have compared the distribution of the $W2400$ equivalent width of UV Fe II emitting quasars in the dense environments of 111 LQGs having $1.1 \leq \bar{z}_{LQG} \leq 1.7$ with the distribution for quasars that are not in LQGs. We find a marginally significant shift (p-value = 0.0226, shift = 0.62 Å) of the $W2400$ distribution to higher values for quasars within LQGs. The shift appears to be a stronger effect at fainter magnitudes $18.0 \leq i \leq 19.1$ (p-value = 0.0064, shift = 0.84 Å).
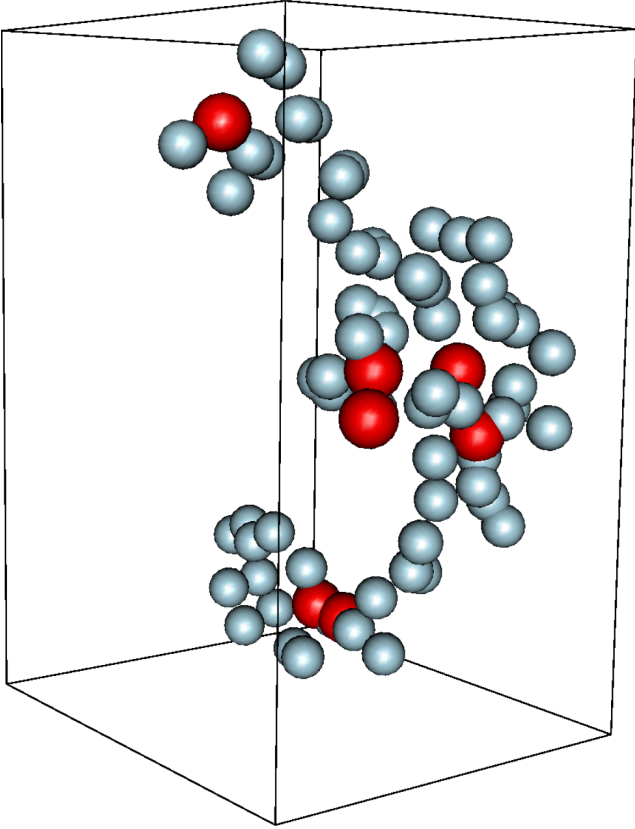
Figure 7. Visualization of the location of the seven ultrastrong-plus emitters ($W2400 \geq 44$ Å) within U1.27, the Huge-LQG. The LQG has 73 members. 66 of the members are represented by spheres of radius that corresponds to 33 Mpc (present epoch). The seven ultrastrong-plus quasars are represented by slightly larger spheres of radius that corresponds to 40 Mpc. The long dimension of the surrounding box corresponds to approximately 1000 Mpc.

However, the shift to higher $W2400$ appears to be strongly concentrated in the 75 LQGs having $1.1 \leq \bar{z}_{\mathrm{LQG}} \leq 1.5$ (p-value = 0.0042, shift = 0.97 Å), and again it appears to be a stronger effect at fainter magnitudes $18.0 \leq i \leq 19.1$ (p-value = 0.00054, shift = 1.31 Å).

We have investigated the distribution of nearest-neighbour separations for the ultrastrong emitters within the 75 LQGs having $1.1 \leq \bar{z}_{\mathrm{LQG}} \leq 1.5$ compared with the distribution for the weak emitters. The nearest neighbours were determined without regard for the strength of their UV Fe ɪɪ emission. We found a marginally significant result (p-value = 0.0255) that the CDF of the ultrastrong ($W2400 \geq 45$ Å) distribution is greater than the CDF of the weak ($W2400 < 30$ Å) distribution. There appears to be a preferred nearest-neighbour separation predominantly in the range ∼25–50 Mpc. We found that a post-hoc adjustment from ultrastrong $W2400 \geq 45$ Å to 'ultrastrong plus' $W2400 \geq 44$ Å gives improved significance (p-value = 0.0197), and a preferred nearest-neighbour separation that then appears to be predominantly in the range ∼30–50 Mpc.

Our finding of a shift towards higher values of $W2400$ for quasars within LQGs is compatible with the result from Harris (2011) and Harris et al. (2012) of a shift for a deep pencil-beam field that intersects the three LQGs U1.11, U1.28 and U1.54 (the doubtful LQG). Our shift seems smaller, but we do find an indication that the shift will increase to fainter magnitudes. The MMT/Hectospec data used by Harris (2011) and Harris et al. (2012) are for quasars

that are typically much fainter than those used here, so it may be that the size of the shifts can still be reconciled. However, there is an inevitable difficulty in constructing a matching control sample for the faint MMT/Hectospec sample, so possibly the attempted allowance for the differences has not been wholly successful and the size of the shift there then appears larger than it should be. We find that the shift is strongly concentrated in the range $1.1 \leq \bar{z}_{\mathrm{LQG}} \leq 1.5$. U1.54 is excluded from our data by this condition of course, but fundamentally it is excluded because it fails our CHMS-significance criterion.

Clowes & Harris (unpublished visualization) noted, for the pencil-beam field within U1.11, U1.28 and U1.54, a tendency for strong/ultrastrong emitters to clump with other quasars or with themselves. With the data for the 75 LQGs having $1.1 \leq \bar{z}_{\mathrm{LQG}} \leq 1.5$ in this paper we find evidence that ultrastrong-plus emitters – those with $W2400 \geq 44$ Å – have a preferred nearest-neighbour scale of ∼30–50 Mpc. This result supports, and makes quantitative, the result from the visualization. However, no such preferred scale is seen for ultrastrong-plus emitters that are not in LQGs.

Our visualization of the ultrastrong-plus emitters across U1.11, U1.28 and U1.54 in their entireties, together with U1.27, is generally consistent with the deeper pencil-beam visualization but not so clear. A striking result, however, is from U1.27, the Huge-LQG, for which six of the seven ultrastrong-plus emitters, from amongst the total of 73 LQG members, form three pairings.

We have thus found two effects of the dense LQG environment on the UV Fe ɪɪ emission of the member quasars. First, there is a general shift to higher $W2400$, compared with non-members for $1.1 \leq \bar{z}_{\mathrm{LQG}} \leq 1.5$. The shift appears to be stronger for fainter magnitudes. This redshift dependence, $\bar{z}_{\mathrm{LQG}} \leq 1.5$, suggests an evolutionary effect. Secondly, we find evidence for a preferred nearest-neighbour separation of ∼30–50 Mpc for the ultrastrong ($W2400 \geq 45$ Å) or, more precisely, ultrastrong-plus ($W2400 \geq 44$ Å) emitters compared with the weak ($W2400 < 30$) emitters within these LQGs. This preferred separation suggests a clustering or dynamical effect. Of course, there may be further subtleties present in the dependences on redshift, magnitude and density than we have seen, but a still larger sample with which to disentangle them is not currently feasible. It may be, however, that a different approach on the existing data, such as fitting templates to the Fe ɪɪ, could restore some information that might presently be lost to uncertainties in measuring $W2400$.

The possibilities for increasing the strength of the Fe ɪɪ emission appear to be Fe abundance, Lyα fluorescence and microturbulence. Probably all of these operate. The dense environment of the LQGs and an increased rate of interactions and mergers between galaxies may have led to an increased rate of star formation and an enhanced abundance of Fe in the nuclei of galaxies. Similarly, the dense environment of the LQGs may have led to more active blackholes and increased Lyα emission. The preferred nearest-neighbour separation for the stronger emitters would appear to suggest a dynamical component, such as microturbulence.

This research has used the SDSS DR7QSO catalogue (Schneider et al. 2010).

REFERENCES

Baldwin J. A., Ferland G. J., Korista K. T., Hamann F., LaCluyzé A., 2004, ApJ, 615, 610

Bruhweiler F., Verner E., 2008, ApJ, 675, 83

Clowes R. G., Campusano L. E., 1991, MNRAS, 249, 218

Clowes R. G., Campusano L. E., Graham M. J., Söchting I. K., 2012, MNRAS, 419, 556

Clowes R. G., Harris K. A., Raghunathan S., Campusano L. E., Söchting I. K., Graham M. J., 2013, MNRAS, 429, 2910

Collin-Souffrin S., Lasota J.-P., 1988, PASP, 100, 1041

Graham M. J., Clowes R. G., Campusano L. E., 1996, MNRAS, 279, 1349

Harris K. A., 2011, PhD thesis, Univ. Central Lancashire

Harris K. A., Clowes R. G., Williger G. M., Haberzettl L. G., Campusano L. E., 2012, in Boissier S., de Laverny P., Nardetto N., Samadi R., Valls-Gabaud D., Wozniak H., eds, SF2A-2012: Proc. Annu. Meeting French Soc. Astron. Astrophys., p. 469

Meusinger H., Schalldach P., Scholz R.-D., in der Au A., Newholm M., de Hoon A., Kaminsky B., 2012, A&A, 541, A77

Newman P. R., 1999, PhD thesis, Univ. Central Lancashire

Newman P. R., Clowes R. G., Campusano L. E., Graham M. J., 1998, in Müller V., Gottlöber S., Mücket J. P., Wambsganss J., eds, Large-Scale Structure: Tracks and Traces. World Scientific, Singapore, p. 133

Penston M. V., 1987, MNRAS, 229, 1p

Richards G. T. et al., 2006, AJ, 131, 2766

Ruff A. J., Floyd D. J. E., Webster R. L., Korista K. T., Landt H., 2012, ApJ, 754, 18

Schneider D. P. et al., 2010, AJ, 139, 2360

Shen Y. et al., 2011, ApJS, 194, 45

Sigut T. A. A., Pradhan A. K., 1998, ApJ, 499, L139

Sigut T. A. A., Pradhan A. K., 2003, ApJS, 145, 15

Vanden Berk D. E. et al., 2005, AJ, 129, 2047

Weymann R. J., Morris S. L., Foltz C. B., Hewett P. C., 1991, ApJ, 373, 23

Wills B. J., Netzer H., Wills D., 1985, ApJ, 288, 94

Zhang X.-G., 2011, ApJ, 741, 104

This paper has been typeset from a TEX/LATEX file prepared by the author.